85-1817

EFFECT OF MAXIMUM LIFT TO DRAG RATIO ON OPTIMAL AEROASSISTED PLANE CHANGE

Jennie R. Johannesen* and Nguyen X. Vinh†
Department of Aerospace Engineering
The University of Michigan
Ann Arbor, Michigan 48109-2140

and

Kenneth D. Mease‡
Jet Propulsion Laboratory
Pasadena, California 91109

Abstract

The influence of the maximum lift-to-drag ratio on the turning performance of an Orbital Transfer Vehicle is analyzed. Chapman's variables are used to formulate the equations of motion which are valid for both atmospheric flight and flight in a vacuum in a Newtonian gravitational field. Of the six adjoint variables involved in the variational formulation we obtain four exact integrals and two approximate relations. This leads to an approximate but explicit control law for the lift and bank control. The control law is tested numerically for a whole range of entry speeds from parabolic entry to near circular entry with several values of maximum lift-to-drag ratio. The extensive numerical results, which are very accurate as compared to the exact optimal values, show that the maximum plane change for any speed ratio V_{entry}/V_{final} is simply proportional to the maximum lift-to-drag ratio and depends solely on this parameter.

Nomenclature

A,B,C = functions as defined in Eq. (25)
C_D = drag coefficient
C_D* = drag coefficient at maximum lift-to-drag ratio
C_{D_o} = zero-lift drag coefficient
C_L = lift coefficient
C_L* = lift coefficient at maximum lift-to-drag ratio
c_i = constants of integration
E* = maximum lift-to-drag ratio
g = gravitational acceleration
H = Hamiltonian
h = altitude
i = inclination
J = performance index
K = induced drag factor
k = Chapman's atmospheric parameter (k = 30 for Earth's atmosphere)
k_i = constant parameters in bank control
m = mass of the vehicle
p_x = adjoint variable associated to state variable x
R = radial distance to entry altitude
r = radial distance to vehicle
S = reference area
s = dimensionless arc length
t = time
u = square of dimensionless speed, Eq. (1)
V = speed
Z = dimensionless density of atmosphere used as altitude variable, Eq. (1)
β = inverse of scale height in exponential atmosphere
γ = flight path angle
θ = longitude
λ = C_L/C_L*, lift control
ρ = density of atmosphere
σ = bank angle
ϕ = latitude
ψ = heading

Subscripts

e = entry condition
f = final condition

Introduction

During the past two decades, considerable effort has been expended to convincingly prove that the use of aerodynamic forces to assist in the orbital transfer can significantly reduce the fuel consumption as compared to the pure propulsive mode. An excellent review of aeroassisted orbit transfer covering an extensive literature has been presented by Walberg.[1] As is usually the case for pioneering work, up to now the authors have concentrated their efforts on the cases where the use of atmospheric passages is clearly advantageous. These are the cases of transfer from a high orbit to a low orbit, and of transfer between non coplanar circular orbits with large plane change.

Future research will certainly cover the general case of transfer from an arbitrary elliptic orbit to another non coplanar orbit using atmospheric turning in the middle portion of the trajectory to reduce the total characteristic velocity (which is a measure of the fuel consumption for high-thrust propulsion system). The overall optimization is a complex problem because there is coupling between the space maneuver and the atmospheric maneuver as shown in Fig. 1.

The initial phase of aeroassisted maneuver is the deorbit phase in which one or two impulses can be used to bring about entry of the Orbital Transfer Vehicle (OTV) into the atmosphere at a certain speed V_e and entry angle γ_e. In this phase a plane change can be achieved. With the two-

---

* Presently, Member of Technical Staff, Jet Propulsion Laboratory

† Professor of Aerospace Engineering

‡ Member of Technical Staff, Member AIAA

impulse deorbit scheme (which may be required because of the geometric configuration of the initial and final orbits) the first impulse is usually used to boost the OTV into a higher orbit where some orbital plane change can be efficiently accomplished during the application of the second impulse. This maneuver is also designed to increase the entry speed for achieving more atmospheric plane change.

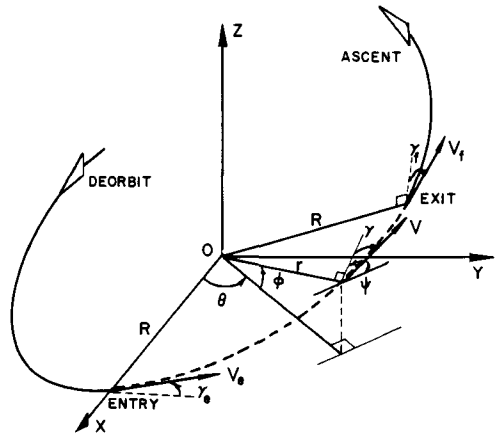

Fig. 1. Aeroassisted maneuver. Nomenclature.

The second phase is the atmospheric turning. In this phase the OTV, which has stored kinetic energy due to high entry speed, can use lift and bank modulation to achieve a major part of the plane change required in the orbital transfer and to exit at a position and with a velocity vector most appropriate for ascending into the final orbit. The final phase is accomplished propulsively with one or two impulses to put the OTV into the final orbit.

We notice that during the space maneuver the fuel consumption occurs at the initial and the final phases. The initial maneuver determines the entry position and velocity, while the final maneuver depends on the exit position and velocity. Therefore a complete analysis of the atmospheric turning phase is required in order to optimize the combined propulsive-atmospheric maneuver. For a three-dimensional maneuver involving a plane change the optimal atmospheric turning consists of finding the lift and bank modulation to bring the vehicle from the initial speed V_e at entry to the final speed V_f at exit such that a maximum plane change is achieved. It will be shown that this turning capability depends on the maximum lift-to-drag ratio of the vehicle. It is proposed in this paper to provide a qualitative and quantitative analysis of this dependence. The numerical data obtained can be tabulated and stored for use in a preliminary design and mission analysis of future OTV's.

Optimal Atmospheric Turning

For a smooth transition from atmospheric flight to flight in the vacuum, or vice versa, it is convenient to use the modified Chapman variables[2]

$$Z = \frac{\rho S C_L^*}{2m}\sqrt{\frac{r}{\beta}} \quad , \quad u = \frac{V^2}{gr} \tag{1}$$

to represent the altitude and the speed variable, and the dimensionless arc length

$$s = \int_0^t \frac{V}{r}\cos\gamma \, dt \tag{2}$$

to replace the time as independent variable. The notation used is the standard notation. The drag polar considered is the parabolic drag polar

$$C_D = C_{D_o} + K C_L^2 \tag{3}$$

with the condition at maximum lift-to-drag ratio

$$C_L = C_L^* = \sqrt{C_{D_o}/K} \quad , \quad C_D = C_D^* = 2C_{D_o}$$

$$(L/D)_{max} = E^* = 1/2\sqrt{KC_{D_o}} \tag{4}$$

Then with a Newtonian gravitational field and a locally exponential atmosphere such that

$$d\rho = -\beta \rho \, dr \tag{5}$$

where the inverse of the scale height β may be allowed to vary with the altitude, we have the universal dimensionless equations of motion[2]

$$\begin{aligned}
\frac{dZ}{ds} &= -k^2 Z \tan\gamma \\
\frac{du}{ds} &= -\frac{kZu(1+\lambda^2)}{E^*\cos\gamma} - (2-u)\tan\gamma \\
\frac{d\gamma}{ds} &= \frac{kZ\lambda\cos\sigma}{\cos\gamma} + 1 - \frac{1}{u} \\
\frac{d\theta}{ds} &= \frac{\cos\psi}{\cos\phi} \\
\frac{d\phi}{ds} &= \sin\psi \\
\frac{d\psi}{ds} &= \frac{kZ\lambda\sin\sigma}{\cos^2\gamma} - \cos\psi\tan\phi
\end{aligned} \tag{6}$$

In these equations the aerodynamic control is represented by the bank angle σ and by the lift coefficient normalized with respect to the lift coefficient at maximum lift-to-drag ratio,

$$\lambda = C_L/C_L^* \tag{7}$$

The equations lead to Keplerian motion in the vacuum when $Z \to 0$. Furthermore they clearly have the advantage that the only physical characteristic of the OTV involved is the maximum lift-to-drag ratio, E^*. The results obtained are general in the sense that they are valid for any particular vehicle having the same value for E^*. For the numerical analysis we shall take three values $E^* = 0.375, 0.75, 1.5$ which are typical for vehicles with low, medium and high maximum lift-to-drag ratio. The characteristic of the atmosphere is specified by the value $k^2 = \beta r$ called Chapman's atmospheric parameter. For the Earth's atmosphere we take the value $k^2 = 900$.

The optimal control problem consists of finding the aerodynamic lift and bank control, λ and σ, as functions of the time to bring the vehicle from the initial entry condition

$$\theta_e = \phi_e = \psi_e = 0,\ Z_e = 0.0002,\ \gamma_e, u_e \text{ prescribed} \tag{8}$$

to the final exit condition

$$Z_f = Z_e\ ,\quad u_f = \text{prescribed} \tag{9}$$

such that the plane change i_f is maximized. Hence, we maximize the function

$$J = -\cos i_f = -\cos \phi_f \cos \psi_f \tag{10}$$

In this problem the final position in terms of the longitude θ_f and latitude ϕ_f is not prescribed. Also we assume that the final exit angle γ_f is free. The initial value Z_e of Z is taken such that at that altitude the sensible atmosphere is encountered.

Using the maximum principle, we introduce the adjoint variables p_x to form the Hamiltonian

$$H = -k^2 Z\, p_Z \tan\gamma - p_u \left[\frac{kZu(1+\lambda^2)}{E^* \cos\gamma} + (2-u)\tan\gamma\right]$$
$$+ p_\gamma\left[\frac{kZ\lambda\cos\sigma}{\cos\gamma} + 1 - \frac{1}{u}\right] + p_\theta \frac{\cos\psi}{\cos\phi} + p_\phi \sin\psi \tag{11}$$
$$+ p_\psi\left[\frac{kZ\lambda\sin\sigma}{\cos^2\gamma} - \cos\psi\tan\phi\right]$$

The maximization of the Hamiltonian with respect to the controls λ and σ leads to the optimal law

$$\lambda\cos\sigma = \frac{E^* p_\gamma}{2up_u}\ ,\quad \lambda\sin\sigma = \frac{E^* p_\psi}{2up_u\cos\gamma} \tag{12}$$

which depends on the adjoint variables. These adjoint components p_x satisfy the adjoint equations

$$\frac{dp_x}{ds} = -\frac{\partial H}{\partial x} \tag{13}$$

where x is any one of the six state variables. It is known that the problem has the following integrals[2]

$$H = c_0,\ p_\theta = c_1,\ p_\phi = c_2\sin\theta - c_3\cos\theta$$
$$p_\psi = c_1\sin\phi + (c_2\cos\theta + c_3\sin\theta)\cos\phi \tag{14}$$

where the c_i are constants of integration. Since the final arc length s_f and final longitude θ_f are not prescribed, we have the transversality condition

$$c_0 = 0\ ,\quad c_1 = 0 \tag{15}$$

With the 4 integrals, we have two more adjoint equations to be integrated. This requires guessing two initial values. With the unknown constants c_2 and c_3 to be chosen we have 4 arbitrary parameters to be selected to match the final and transversality conditions. By normalizing the adjoint variables we are left with a 3-parameter problem. The problem has been solved in Ref. 3 with the value E* = 1.5 for the OTV. As is well known, this numerical method of solution is not an easy task due to the high sensitivity of the parameters to be selected. In the following, we will first reduce the order of the system so that we can evaluate approximately the two remaining adjoint variables and obtain an approximate but explicit aerodynamic control law containing only 2 constant parameters. Then using this control law to integrate the exact equations, we obtain the plane change for each speed reduction. The results are very close to exact solution obtained through much laborious procedure. Furthermore, from the explicit form of the control, its behavior can be established.

Optimal Lift and Bank Modulation

The atmospheric trajectory is essentially a skip trajectory at small flight path angle. This angle varies slowly so that we have $d\gamma/ds \approx 0$. From the equation for γ in system (6) we obtain the so-called equilibrium glide solution

$$kZ\lambda\cos\sigma = \frac{(1-u)}{u}\cos\gamma \tag{16}$$

Using this condition, we rewrite the system

$$\frac{du}{ds} = -\frac{(1+\lambda^2)(1-u)}{E^*\lambda\cos\sigma} - (2-u)\tan\gamma$$
$$\frac{d\theta}{ds} = \frac{\cos\psi}{\cos\phi}$$
$$\frac{d\phi}{ds} = \sin\psi \tag{17}$$
$$\frac{d\psi}{ds} = \frac{(1-u)}{u\cos\gamma}\tan\sigma - \cos\psi\tan\phi$$

In this system γ has an average constant value since the equation for γ is satisfied identically. With regard to the lift control we consider the first term of the Hamiltonian containing λ

$$H = -p_u\frac{(1+\lambda^2)(1-u)}{E^*\lambda\cos\sigma} + \ldots \tag{18}$$

The maximization of the Hamiltonian with respect to λ leads to the condition

$$\lambda^2 = 1,\ \frac{\partial^2 H}{\partial\lambda^2} = -\frac{2p_u(1-u)}{E^*\lambda^3\cos\sigma} = -\frac{2p_u(1-u)}{E^*\lambda\cos\sigma} < 0 \tag{19}$$

In this reduced model the lift control is at maximum lift to drag ratio, $\lambda = \pm 1$. We shall take $\lambda = +1$ and allow the bank angle to exceed 90° in the case where the lift is pointing downward. It is seen from the condition (19) that for $p_u > 0$, at supercircular speed (u>1) we must have $\cos\sigma < 0$ and $\sigma > 90^\circ$. On the other hand, at subcircular speed (u<1) $\sigma < 90^\circ$ and a positive vertical component of the lift, $\lambda\cos\sigma > 0$, is required to complete the turning skip.

At this point, it should be noticed that the equilibrium glide assumption (16) and the reduced system (17) have been solely used to deduce the suboptimal law $\lambda \approx 1$ for the lift control. We now return to the complete Hamiltonian (11) to obtain the optimal modulation of the bank angle. Using this Hamiltonian to write Eq. (13) for the adjoint p_Z, we have

$$\frac{dp_Z}{ds} = k^2 p_Z \tan\gamma + p_u \frac{ku(1+\lambda^2)}{E^* \cos\gamma}$$

$$- p_\gamma \frac{k\lambda\cos\sigma}{\cos\gamma} - p_\psi \frac{k\lambda \sin\sigma}{\cos^2\gamma} \qquad (20)$$

Combining with the state equation (6) for Z, we obtain

$$\frac{d(Zp_Z)}{ds} = p_u \frac{kZu(1+\lambda^2)}{E^* \cos\gamma} - p_\gamma \frac{kZ\lambda\cos\sigma}{\cos\gamma} - p_\psi \frac{kZ\lambda\sin\sigma}{\cos^2\gamma} \qquad (21)$$

With the control law (12), we have the exact equation

$$\frac{d(Zp_Z)}{ds} = p_u \frac{kZu(1-\lambda^2)}{E^* \cos\gamma} \qquad (22)$$

With the approximate lift control $\lambda^2 = 1$, we have the integral

$$Zp_Z = c_4 \qquad (23)$$

We now write the Hamiltonian integral $H = 0$ with the condition $\lambda = 1$ and use Eqs. (12) to express up_u and p_γ in terms of p_ψ. Then using the integrals (14) and (23) and the transversality condition (15), we obtain the equation for the optimal bank angle

$$A\cos\sigma + B\sin\sigma + C = 0 \qquad (24)$$

where

$$A = \frac{(1-u)}{u}(\cos\theta + k_1 \sin\theta)\cos\phi$$

$$B = (\cos\theta + k_1\sin\theta)\cos\gamma\cos\psi\sin\phi + (k_1\cos\theta - \sin\theta)\cos\gamma\sin\psi + k_2\sin\gamma \qquad (25)$$

$$C = \frac{E^*(2-u)}{2u}(\cos\theta + k_1\sin\theta)\cos\phi\tan\gamma$$

and

$$k_1 = \frac{c_3}{c_2}, \quad k_2 = \frac{k^2 c_4}{c_2} \qquad (26)$$

are two arbitrary constants to be evaluated.

Equation (24) can be transformed into a quadratic equation for $\tan(\sigma/2)$

$$(A-C)\tan^2\frac{\sigma}{2} - 2B\tan\frac{\sigma}{2} - (A+C) = 0 \qquad (27)$$

with the solution

$$\tan\frac{\sigma}{2} = \frac{1}{(A-C)}\left[B \pm \sqrt{A^2+B^2-C^2}\right] \qquad (28)$$

Hence the bank angle is expressed explicitly in terms of the state variables and two constants of integration.

Transversality Condition

As discussed before since we only have 4 exact integrals (14), the numerical solution of the exact formulation requires integrating 2 adjoint equations in addition to the state equations (6). In theory any one of the three unknown adjoints, p_Z, p_u and p_γ can be solved in terms of the other two by using the Hamiltonian integral. In practice, solving for p_Z is not convenient since this variable is not defined when $\gamma = 0$ at the bottom of the trajectory. On the other hand, solving for p_γ or p_u from the Hamiltonian integral requires the solution of a quadratic equation with some difficulty during the integration because of the square root involved. Therefore, the approach used in Ref. 3 has been the integration of three adjoint equations with the Hamiltonian integral used for checking the accuracy of the numerical solution. The main difficulty in this method of solution has been the sensitivity of the 3 constant parameters which must be adjusted to match the final and transversality condition.

In the present formulation we have explicit control laws for the lift and bank modulation. Furthermore there are only two constant parameters k_1 and k_2 involved, and only the state equations need to be integrated. The labor involved for the computation of a large family of trajectories involving several values of maximum lift-to-drag ratio is greatly reduced. Obviously, with only 2 parameters, one transversality condition is not satisfied. To obtain the best trajectory we shall neglect the least sensitive condition.

From the terminal conditions (8) and (9), and the performance index (10), we see that for a three-parameter problem we can use the exit conditions on u_f, γ_f and ϕ_f to adjust the parameters. In aeroassisted transfer the atmospheric plane change is usually less than 20^o and as such the lateral range ϕ is small. Then $\cos i_f \approx \cos\psi_f$. The final lateral range is not involved in the performance index and can be considered free in the optimization process. Furthermore for small ϕ in the state equations (6) we can make $\cos\phi \approx 1$, and in the equation for ψ we can neglect the centrifugal term, $\cos\psi\tan\phi$ which is small compared to the aerodynamic term. Then, ϕ is ignorable coordinate and $p_\phi = c = 0$. This means that we can neglect the transversality condition involving ϕ_f and use the condition on u_f and γ_f at $Z_f = Z_e$ to adjust the parameters k_1 and k_2 in our control law for the bank angle. Since γ_f is free, $p_\gamma(s_f) = 0$. From the control law (12), this implies that $\cos\sigma_f = 0$, that is

$$\sigma_f = 90^o \qquad (29)$$

Numerical Results

For the numerical computation, we specify a value of maximum lift-to-drag ratio E* and compute the plane change for several values of the entry speed u_e starting with $u_e = 2$ for parabolic entry. Z_e was selected to be a value which corresponds to atmospheric entry with an initial acceleration due to aerodynamic force on the order of $a/g \approx 0.01$. The values for the entry flight path angle were chosen to be small and yet provide for a large atmospheric turning. The constant parameters k_1 and k_2 are selected such that at exit ($Z_f = Z_e$) the final prescribed speed u_f is matched and the transversality condition (29) satisfied. To ease the

computation we simply use k_2 as a scanning parameter. For each k_2 the value of k_1 is adjusted such that condition (29) is matched. The final value u_f obtained is accepted as the prescribed value.

The procedure for determining appropriate values for k_1 and k_2 consists of starting with a rather large negative value for k_2 and adjusting the value of k_1 until the transversality condition (29) is satisfied. More positive k_2 values are then selected which provide smaller exit velocities and larger plane change angles. As an aid in computation the locus of k_1, k_2 values which satisfy the transversality condition (29) may be graphed and used to predict approximately the appropriate value of k_1 (the value for which $\sigma_f = 90^o$) for any given value of k_2. Figure 2 shows such a plot of k_1, k_2 values which satisfy the transversality condition (29) for the case of parabolic entry speed. Figure 3 demonstrates the relationship of the exit speed and resulting plane change angle to k_2 values for the same entry speed.

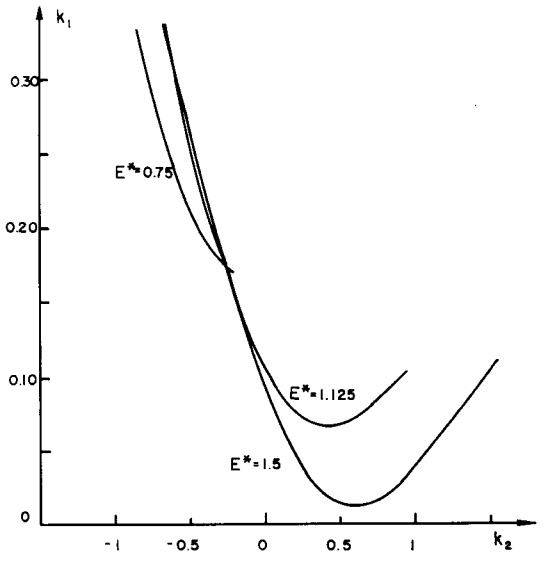

Fig. 2. Plot of k_1 versus k_2 for the case of parabolic entry ($u_e = 2$).

Although the control laws are approximate, the exact state equations (6) are used and therefore we can compare the plane change i_f obtained from the approximate control with the optimal value obtained through modulating both the lift and the bank in the exact formulation. For the value $E^* = 1.5$ extensive data for optimal plane change has been compiled and summarized in Ref. 4. For the same entry and exit speed the value i_f obtained with our proposed control law agrees to within a fraction of one degree with the optimal plane change angles from Ref. 4, even for large plane changes. This close agreement occurs because in

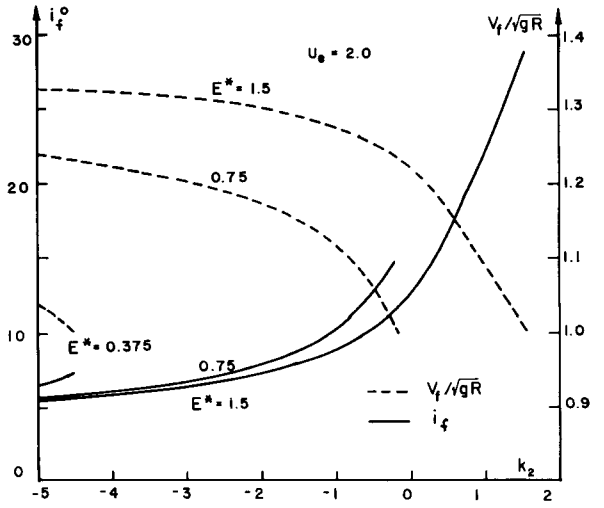

Fig. 3. Relationship between the plane change angle i_f (or final speed V_f) and the parameter k_2 for the case of parabolic entry ($u_e = 2$).

the optimal trajectory the lift control λ is oscillating near the value $\lambda = 1$ used in approximate control and because the behaviors of the bank angle are quite similar to each other. This also leads to a closeness of the trajectory variables when we compare the suboptimal trajectory with the optimal one.

As an example, we consider in Figs. 4 and 5 the trajectory variables for the case of an entry for a return from a geosynchronous orbit with $u_e = 1.733$ and $\gamma_e = -4^o$ with an OTV such that $E^* = 1.5$. With the approximate control we obtain the following results

$$\begin{aligned} V_f/\sqrt{g\,R} &= 1.02827 \quad (1.02893) \\ i_f &= 20.9079^o \quad (20.9057^o) \\ \gamma_f &= 1.5089^o \quad (1.9037^o) \\ \theta_f &= 32.8744^o \quad (28.3869^o) \\ \phi_f &= 7.3151^o \quad (5.9549^o) \\ \psi_f &= 19.6404^o \quad (20.0761^o) \end{aligned}$$

The numbers in parentheses are the final values from the optimal solution. In both cases the exact equations of motion (6) are used so that the two trajectories are the actual trajectories flown. Figure 4 shows the variations of the dimensionless speed $V/\sqrt{g\,R}$ and the altitude drop $-\beta\,\Delta\,h$. The speed is simply $\sqrt{u}$ with the circular speed $\sqrt{g\,R}$ evaluated at entry. As for the altitude drop, from the definition (1) of Z, it is

$$\beta\,\Delta\,h = -\ell n\,(Z/Z_e) \qquad (30)$$

Trajectories from the optimal control are plotted in solid lines while the small circles represent data from trajectories with the present control. The suboptimal trajectory is more extended in the range but the altitude variation is the same. This results in the same management in the speed.

Figure 5 shows the variations of the lateral range, heading and flight path angle. It is seen that in both cases most of the turning is made at low altitude. It is also there that most of the speed depletion occurs. From the figure we detect a slight decrease of the heading near the end of the turning. From the last equation in system (6), it is seen that this occurs when the centrifugal force becomes large and

$$\frac{k\, Z\, \lambda\, \sin\sigma}{\cos^2 \gamma} = \cos\psi \tan\phi \qquad (31)$$

Since theoretically Z is very small at exit, we have this feature on all skip trajectories. On the other hand, since

$$\cos i = \cos\phi \cos\psi \qquad (32)$$

we have by using the state equations (6)

$$\frac{di}{ds} = \frac{k\, Z \cos\phi \sin\psi}{\sin i \cos^2 \gamma}\, \lambda \sin\sigma \qquad (33)$$

Then, it is seen that i increases continuously with $\sin\sigma > 0$.

Figure 6 shows the influence of the maximum lift-to-drag ratio on the turning performance. The entry speed is the parabolic speed $u_e = 2$. For each value of the maximum lift-to-drag ratio E* we have computed and plotted the maximum plane change i_f for each prescribed value of the final dimensionless speed $V_f/\sqrt{gR}$. In a preliminary assessment, it is seen that the maximum plane change is proportional to E*. For an estimate of this performance, we can use the first order solution

$$i_f = \frac{180\ E^*}{\pi} \ln \frac{V_e}{V_f} \qquad (34)$$

This solution is plotted in dashed lines in Fig. 6 and is within 1% of the optimal solution.

The approximate aerodynamic control, $\lambda = 1$ and σ given by Eq. (24), is very accurate and shows the correct behavior of the bank control. This behavior is shown in Fig. 7. At the initial phase the optimal bank angle is high and exceeds 90°. Hence the lift force is directed downward and is used to pull the OTV rapidly toward the dense atmosphere where effective turning is made. For a supercircular speed exit the bank angle decreases toward its final

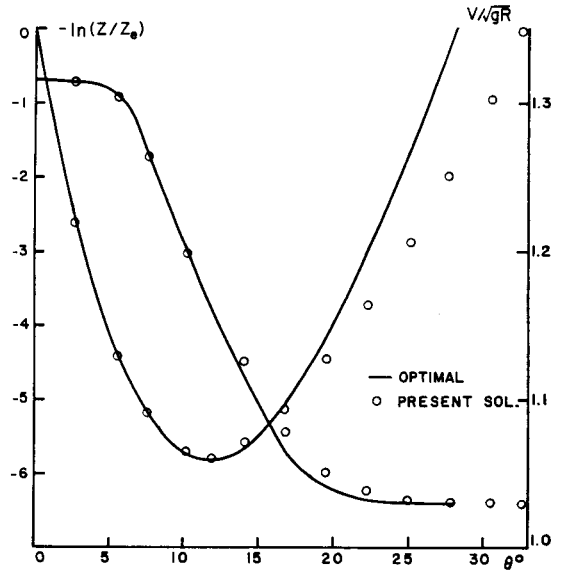

Fig. 4. Variations of the speed and altitude. Case of E* = 1.5, $u_e = 1.733$, $i_f = 20.9^\circ$.

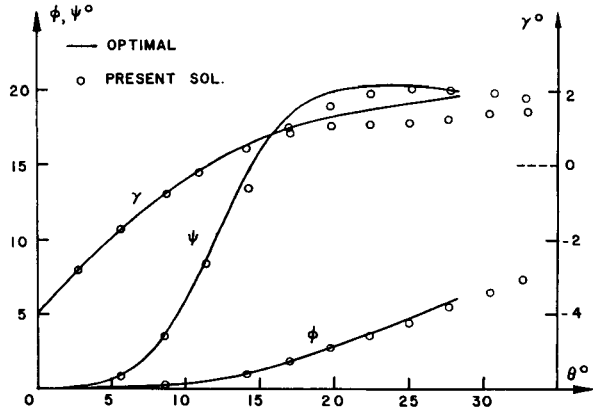

Fig. 5. Variations of the lateral range, heading and flight path angle. Case of E* = 1.5, $u_e = 1.733$, $i_f = 20.9^\circ$

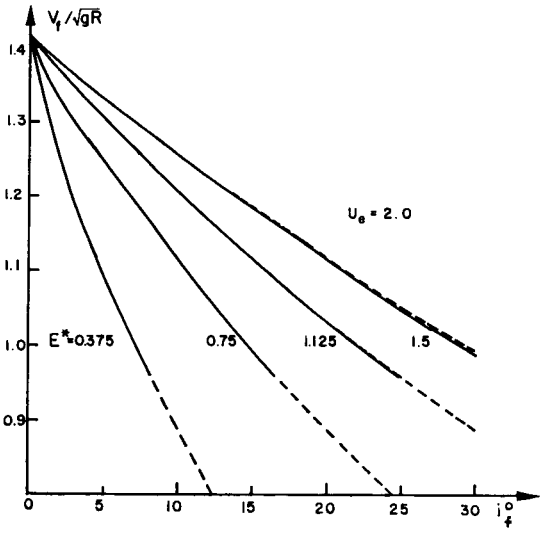

Fig. 6. Maximum plane change as function of the final speed for various values of E*. Case of parabolic entry, $u_e = 2.0$.

optimal value $\sigma_f = 90^o$. The vehicle pulls out on strength of the centrifugal force. On the other hand, for a subcircular exit speed, a positive vertical component of the lift force is required during the climbing phase of skip turning. Then as shown in Fig. 7, the bank angle becomes less than 90^o to produce upward lift. It decreases to a minimum value and in the terminal phase increases to the final value of 90^o.

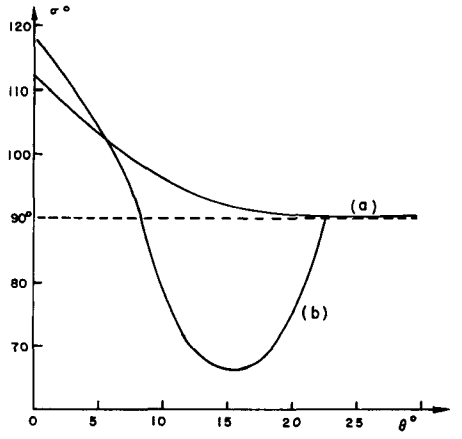

Fig. 7. Variations of the optimal bank angle for exit at: (a) supercircular speed; (b) subcircular speed.

The numerical computation for the whole range of entry speed from parabolic entry to near circular entry for different values of the maximum lift-to drag ratio is fairly routine for supercircular exit speed $V_f/\sqrt{g\,R} > 1$. This is because, as explained above, we need to do an iteration only on one parameter k_1 while using k_2 as a scanning parameter. On the other hand we encounter some mild difficulties for large plane change when the exit speed becomes subcircular. This is because as seen from Eq. (25), A is small when $u \approx 1$ and the discriminant

$$D = A^2 + B^2 - C^2 \qquad (35)$$

in the quadratic formula (28) can be negative. Along the optimal trajectory, the coefficients A, B and C and consequently the bank angle σ are functions of the independent variable s. If D decreases to a minimum value and then increases while remaining positive, the trajectory can be continued until exit or until crashing. Then an iteration can be made to satisfy the transversality condition (29). If negative values of D are encountered, we have the limiting case when the minimum value of D is zero. Then we have at that point

$$D = A^2 + B^2 - C^2 = 0 \qquad (36)$$

and

$$D'/2 = AA' + BB' - CC' = 0 \qquad (37)$$

where the prime denotes the derivative with respect to s. On the other hand, as shown in Fig. 7, the optimal bank angle passes through a minimum for the case of subcircular speed exit. At that point

$$\begin{aligned} A\cos\sigma + B\sin\sigma + C &= 0 \\ A'\cos\sigma + B'\sin\sigma + C' &= 0 \end{aligned} \qquad (38)$$

By eliminating σ between the last two equations, we have the condition at the minimum bank angle

$$(AC' - A'C)^2 + (BC' - B'C)^2 = (AB'-A'B)^2 \qquad (39)$$

It is easy to verify that if the two equations (36) and (37) are satisfied, then condition (39) is also satisfied. Then for subcircular speed exit, for each value of k_2, we first find the value of k_1 such that the two conditions (36) and (37) are satisfied at a certain point on the trajectory. At that point, the bank angle passes through a minimum. We have then the limiting value of k_1 for the bank angle to exhibit the behavior as shown in trajectory (b) of Fig. 7. The optimal trajectory is found by searching for values of k_1 beyond the limiting value, and the difficulty with imaginary roots is avoided.

Since the maximum plane change i_f is essentially proportional to E*, it is possible to plot the results of extensive numerical computation in one single graph as shown in Fig. 8. In this figure we use the square of the dimensionless speed, u_e, as parameter and plot the dimensionless exit speed, $V_f/\sqrt{g\,R}$, versus the ratio i_f/E^*. Then the graph can be used for any value of the maximum lift-to-drag ratio selected.

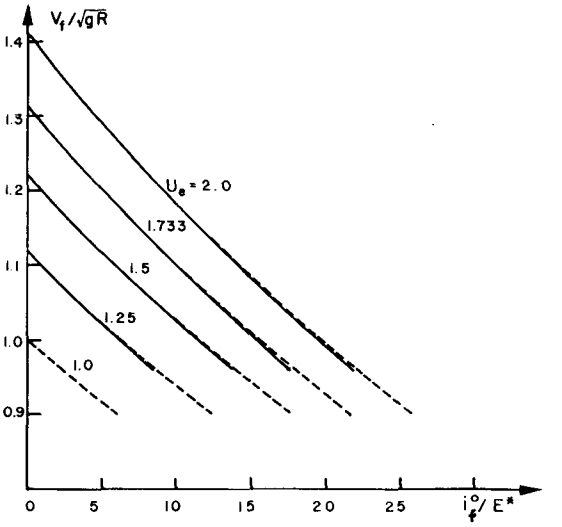

Fig. 8. Maximum plane change angle as function of the exit speed for several values of the entry speed. The graph can be used for any value of E*.

In Fig. 8 we have also plotted Eq. (34) in dashed lines for comparison. To obtain this equation we have used the small angle approximation and neglected the centrifugal term to write the equations for u and ψ in system (6) as

$$\frac{du}{ds} = -\frac{kZu(1+\lambda^2)}{E^*}$$
$$\frac{d\psi}{ds} = k\,Z\,\lambda\,\sin\sigma \qquad (40)$$

Furthermore, we use the approximation $\cos i = \cos\phi\cos\psi \approx \cos\psi$. Then using u as independent variable, we form the equation for constant lift and bank

$$\frac{di}{du} = -\frac{E^*\lambda}{(1+\lambda^2)u}\sin\sigma \qquad (41)$$

which can be integrated to give

$$\frac{i_f}{E^*} = \frac{2\lambda\sin\sigma}{(1+\lambda^2)}\ln\frac{V_e}{V_f} \qquad (42)$$

The maximization of this plane change with respect to the lift control λ and bank angle σ leads to $\lambda = 1$ and $\sigma = 90^o$. Hence we have in radians

$$\frac{i_f}{E^*} = \ln\frac{V_e}{V_f} \qquad (43)$$

which is the same as Eq. (34) expressed in degrees. It should be noticed that this equation is solely used as an excellent estimate of the maximum plane change and as such it is a useful formula to be used in connection with a preliminary optimization of the combined aerodynamic-propulsive maneuver.

Since flight at constant lift coefficient and bank angle is an attractive program, we have investigated the possibility of using this mode as an alternate way of generating suboptimal trajectories for atmospheric plane change. From the previous analysis we consider the case of $\lambda = 1$ and $\sigma = 90^o$. For the numerical analysis, we use $E^* = 1.5$ and $u_e = 1.733$, that is, the case of entry for return from a geosynchronous orbit. First, it should be noticed that if the entry angle is held at a fixed value, say $\gamma_e = -4^o$, then flexibility in controlling the trajectory is lost and from the integration of the exact equations we simply obtain $i_f = 9.18^o$ at an exit speed $V_f/\sqrt{gR} = 1.18202$. On the other hand, the optimal program with modulation of both the lift coefficient and the bank angle or the present program with lift coefficient at maximum lift-to-drag ratio and the bank angle according to Eq. (24) allows the control of the flight from any given entry condition, to any desired final speed with maximum plane change angle. For constant aerodynamic control, in order to obtain various final speeds, and hence different plane change angles, we must vary the entry angle γ_e. This has little influence on the total characteristic velocity in the optimization process since γ_e only varies in a small range. The comparative results are shown in Table 1.

First, we compute the plane change angles i_f obtained with the constant lift and bank program for different entry angles. These are shown in the third column. It is seen that the plane change angle is very sensitive to change in the entry angle. From a value of $\gamma_e = -3.5^o$ leading to $i_f = 2.42^o$, when we increase to $\gamma_e = -4.25^o$, we obtain $i_f = 24.78^o$. This value is about the maximum plane change angle obtained by this mode since when we slightly increase the entry angle to $\gamma_e = -4.255^o$ in order to obtain a higher plane change, we have a crashing trajectory.

Table 1. Comparison of the performances from various flight programs. Case of $E^* = 1.5$, $u_e = 1.733$.

$-\gamma_e$	$V_f/\sqrt{gR}$	$i_f(\lambda=1, \sigma=90^o)$	i_f(opt.)	i_f(sub-opt.)	i_f, Eq.(34)
3.5^o	1.27971	2.41788^o	2.43165^o	2.41958^o	2.43165^o
3.8	1.23922	5.15903	5.12048	5.07473	5.19485
4.0	1.18202	9.18030	9.17059	9.18196	9.25632
4.1	1.13346	12.7456	12.7662	12.7198	12.8617
4.2	1.05497	18.8286	18.8287	18.7311	19.0292
4.225	1.02518	21.2498	21.2203	21.2204	21.4910
4.250	0.98305	24.7791	24.6908	24.7494	25.0979

Next, using various final speeds as shown in the second column, we evaluate the optimal plane change angles as tabulated in Ref. 4 and also compute i_f using the bank control law (24). These trajectories are all computed with the same entry angle $\gamma_e = -4^o$. The results are reported in Table 1 for comparison. Finally, in the last column we provide the estimate of the plane change angle as given by Eq. (34).

It is seen that the results are close to each other, with Eq. (34) giving a slight overestimated value in each case. Rigorously speaking, of the three control laws tested, the one providing i_f(opt) must be the best. Some of the values in the column i_f(subopt) obtained with the bank control proposed in this paper appear slightly higher. This closeness makes explicit the excellent performance of this control law, and the small difference is simply due to the extrapolation we use to analyze data from Ref. 4 for a match with the required final speed.

The constant aerodynamic control program also provides excellent results. This is because, as seen in Fig. 7 for supercircular speed exit, the optimal bank angle is close to 90^o. The higher value used for σ in the initial phase is designed to direct the lift downward to pull the vehicle into the dense layer of the atmosphere where turning at $\sigma = 90^o$ is effectively made. In the constant bank program, this is aided by selecting a steeper entry angle. Some plane change angles in this mode appear higher than the optimal values. This is because in the optimal program we keep γ_e fixed at -4^o. If we search for the best entry angle, then the value i_f(opt) obtained will be the overall best value for the same exit speed. But since this only gives a slight improvement, and in the optimal program we deal with the iteration on three parameters and in the suboptimal program, two parameters are involved, in order to obtain extensive data for various entry speeds with different values of the maximum lift-to-drag ratio, the entry angle has not been used as

additional parameter in the computation.

In summary, for a prescribed entry condition, optimal modulation of both the lift coefficient and the bank angle is required to bring the vehicle to the desired exit speed with maximum plane change. As a suboptimal solution, the lift coefficient can be kept at its value for maximum lift-to-drag ratio, while the bank angle is controlled according to the explicit formula (24) with comparable results. Flight at maximum lift-to-drag ratio and 90° bank angle can be used to obtain near optimal plane change angle for any desired supercircular exit speed and this is through the appropriate selection of the entry angle. This would require accurate guidance of the deorbit trajectory since in the constant bank angle mode the plane change angle is very sensitive to the variation of the entry angle.

As a final remark, turning at $\sigma = 90^{\circ}$ eliminates a lift component in the normal direction in the osculating plane, that is the $(\vec{r},\vec{V})$ plane. Then, as far as the altitude, flight path angle and speed are concerned, that is for the variables Z, γ and u, their equations are the same as the equations in planar ballistic flight. This problem of ballistic fly-through has been investigated in detail in Ref. 5 and it has been found that for a given entry speed, entry altitude and ballistic coefficient, there exists a critical entry angle beyond which the vehicle fails to exit. At this critical entry angle, the ballistic trajectory leads to an exit speed slightly subcircular. An accurate formula for the evaluation of this critical angle has been provided in Ref. 5. In terms of the notation used in this paper, it is

$$\frac{1.67\ Z_e}{E^*}\sqrt{\frac{2(u_e-1)\,\pi}{u_e}}\ \exp\left[\frac{k^2 u_e \sin^2\gamma_e}{2(u_e-1)}\right]$$

$$= \frac{1}{u_e} - 1 + \ln u_e \qquad (44)$$

For the case in Table 1, with $u_e = 1.733$, $Z_e = 0.0002$ and $E^* = 1.5$ we obtain from this formula $\gamma_e = 4.2549^{\circ}$. This is the same value we have found in our numerical analysis. Turning at 90° bank angle cannot be achieved beyond this entry angle and the plane change angle with this mode is restricted at $i_f < 24.78^{\circ}$, $V_f/\sqrt{gR} > 0.983$.

Conclusion

In this paper we have analyzed the influence of the maximum lift-to-drag ratio E* on the turning performance of an Orbital Transfer Vehicle. Chapman's variables are used to formulate the equations of motion which are valid for both atmospheric flight and flight in a vacuum in a Newtonian gravitational field. Using the variational method for the six adjoint equations, we obtain four exact integrals and two approximate relations. This leads to an approximate but explicit control law for the lift and bank control. The control law is tested numerically for a whole range of entry speed from parabolic entry to near circular entry with several values of maximum lift-to-drag ratio. It is observed that the maximum plane change for any speed ratio V_e/V_f is simply proportional to the maximum lift-to-drag ratio and depends solely on this parameter. The analysis, which is summarized in an explicitly displayed graph, should be useful for a preliminary design and mission analysis of future OTV's.

Acknowledgement

This work was supported by the Jet Propulsion Laboratory under contract No. 956416.

References

1. Walberg, G.D., "A Survey of Aeroassisted Orbit Transfer," AIAA J. Spacecraft. Vol. 22, No. 1, Jan.-Feb. 1985, pp. 3-18.

2. Vinh, N.X., "Optimal Trajectories in Atmospheric Flight." Elsevier Scientific Publishing Co., Amsterdam and New York, 1981.

3. Vinh, N.X., and J.M. Hanson, "Optimal Aeroassisted Return From High Earth Orbit with Plane Change," Acta Astronautica, to appear.

4. Hanson, J.M., "Optimal Maneuvers of Orbital Transfer Vehicles," Ph.D. dissertation, The University of Michigan, 1983.

5. Vinh, N.X., Johannesen, J.R., Longuski, J.M., and J.H. Hanson, "Second-Order Analytic Solutions for Aerocapture and Ballistic Fly-Through Trajectories," The Journal of the Astronautical Sciences, Vol. 32, No. 4, Oct.-Dec. 1984, pp. 429-445.